Crystal Structure of the Topoisomerase II Poison 9-Amino-[*N*-(2-dimethylamino)ethyl]acridine-4-carboxamide Bound to the DNA Hexanucleotide d(CGTACG)$_2$[†]

Adrienne Adams,* J. Mitchell Guss, and Charles A. Collyer

Department of Biochemistry, University of Sydney, NSW 2006, Australia

William A. Denny

Auckland Cancer Society Research Centre, Faculty of Medicine and Health Science, The University of Auckland, Private Bag 92019, Auckland, New Zealand

Laurence P. G. Wakelin

School of Chemistry and the School of Physiology and Pharmacology, University of New South Wales, NSW 2052, Australia

Received February 12, 1999; Revised Manuscript Received April 29, 1999

ABSTRACT: The structure of the complex formed between d(CGTACG)$_2$ and the antitumor agent 9-amino-[*N*-(2-dimethylamino)ethyl]acridine-4-carboxamide has been solved to a resolution of 1.6 Å using X-ray crystallography. The complex crystallized in space group $P6_4$ with unit cell dimensions $a = b = 30.2$ Å and $c = 39.7$ Å, $\alpha = \beta = 90°$, $\gamma = 120°$. The asymmetric unit contains a single strand of DNA, 1.5 drug molecules, and 29 water molecules. The final structure has an overall *R* factor of 19.3%. A drug molecule intercalates between each of the CpG dinucleotide steps with its side chain lying in the major groove, and the protonated dimethylamino group partially occupies positions close to (∼3.0 Å) the N7 and O6 atoms of guanine G2. A water molecule forms bridging hydrogen bonds between the 4-carboxamide NH and the phosphate group of the same guanine. Sugar rings adopt the C2′-*endo* conformation except for cytosine C1 which moves to C3′-*endo*, thereby preventing steric collision between its C2′ methylene group and the intercalated acridine ring. The intercalation cavity is opened by rotations of the main chain torsion angles α and γ at guanines G2 and G6. Intercalation perturbs helix winding throughout the hexanucleotide compared to B-DNA, steps 1 and 2 being unwound by 8° and 12°, respectively, whereas the central TpA step is overwound by 17°. An additional drug molecule, lying with the 2-fold axis in the plane of the acridine ring, is located at the end of each DNA helix, linking it to the next duplex to form a continuously stacked structure. The protonated *N,N*-dimethylamino group of this "end-stacked" drug hydrogen bonds to the N7 atom of guanine G6. In both drug molecules, the 4-carboxamide group is internally hydrogen bonded to the protonated N-10 atom of the acridine ring. The structure of the intercalated complex enables a rationalization of the known structure−activity relationships for inhibition of topoisomerase II activity, cytotoxicity, and DNA-binding kinetics for 9-aminoacridine-4-carboxamides.

DNA intercalating agents that form ternary complexes with mammalian topoisomerases and poison their cleavage and rejoining activities are important in the treatment of cancer (*1, 2*). The most prominent examples in general clinical use are the anthracycline antibiotics adriamycin and daunomycin, the anthracenedione mitoxantrone, and the antileukemic 9-anilinoacridine amsacrine (*1*). The search for analogues of amsacrine active against solid tumors lead Denny and colleagues to synthesize the 4-methyl-5-methylcarboxamide derivative, asulacrine (CI-921) (*3*), which has undergone phase II clinical trials (*4, 5*). Further work with acridinecarboxamide derivatives revealed that 9-aminoacridine-4-carboxamides (see Figure 1) are also potent cytotoxins and that they have high activity against mouse leukemia models in vivo (*6*−*8*). The des-9-amino derivative, designated DACA[1] (NSC 601316), shows inhibitory activity against both topoisomerase I (*9*) and topoisomerase II (*10*), and is currently in clinical trial (*11*−*13*). DACA has a wide spectrum of activity against solid tumors in animals (*11, 14*), and is relatively unaffected by P-glycoprotein-mediated multidrug resistance, probably due to its high lipophilicity (*15*).

The parent compound 9-amino-DACA (Figure 1) is a dication at neutral pH (pK_as of 8.3 and 10, see ref *8*); it intercalates into DNA with an unwinding angle of 17° (*16*)

[†] This work was funded by The Association for International Cancer Research, Grants 96/41 and 98/288.

* To whom correspondence should be addressed.

[1] Abbreviations: DACA, *N*-[2-(dimethylamino)ethyl]acridine-4-carboxamide; 9-amino-DACA, 9-amino-[*N*-(2-dimethylamino)ethyl]acridine-4-carboxamide; 6-Br-9-amino-DACA, 9-amino-6-bromo-[*N*-(2-dimethylamino)ethyl]acridine-4-carboxamide; MPD, 2-methyl-2,4-pentanediol; NOE, nuclear Overhouser effect; RMSD, root-mean-square deviation; HPLC, high-pressure liquid chromatography; MAD, multiwavelength anomalous dispersion.

10.1021/bi990352m CCC: $18.00
Published on Web 06/26/1999

and has an affinity of 4×10^5 M^{-1} for calf thymus DNA in 100 mM NaCl at pH 7.0 (*17*). It preferentially binds to GC-rich nucleotide sequences (*7*, *18*) and selectively poisons topoisomerase II (*9*, *19*). There are tight correlations between ligand structure, cytotoxicity, and DNA-binding kinetics for the 9-aminoacridine-4-carboxamide class of compounds (*6*−*8*, *19*, *20*). The most notable features of the structure−activity relationships are that the side chain must be in the acridine 4-position, that the carboxamide must have an unsubstituted NH group, and that there must be two methylene groups between the carboxamide NH and the terminal protonated *N*,*N*-dimethylamino group (*6*). These findings, coupled with the dependence of the dissociation kinetics profile on ligand structure (*20*), imply that the side chain makes specific interactions with the DNA that are sensed by topoisomerase II in the ternary complex. Accordingly, the kinetic data have been interpreted in terms of a binding model in which the drug intercalates at CpG sequences and the 4-carboxamide side chain lies in the minor groove with the carboxamide and protonated *N*,*N*-dimethylammonium groups making hydrogen bonding interactions with a cytosine O2 oxygen atom (*20*). However, this proposal has been challenged several times, and on the basis of a variety of molecular modeling approaches, Chen et al. (*21*), Hudson et al. (*22*) and Rehn and Pindur (*23*) suggest that the side chain lies in the major groove at CpG dinucleotides, making hydrogen bonding interactions with the guanine O6 and N7 atoms.

Direct experimental attempts to determine which groove the 4-carboxamide side chain lies in using NMR spectroscopy have, to date, proven unsuccessful because 9-amino-DACA complexes with short oligonucleotides are in fast or intermediate exchange on the NMR time scale which makes it difficult to observe intermolecular NOEs (*24*, Wakelin, unpublished observations). The results of indirect methods based upon the ability of the bound ligand to inhibit the activity of DNase I (*18*) or to bind to DNA in which the major groove is occluded by glycosylation or the minor groove blocked by distamycin (*17*) have been interpreted to imply that the side chain is located in the minor groove. To help resolve the uncertainty of the binding orientation of the acridine-4-carboxamides, we have initiated a crystallographic study of their interaction with DNA hexanucleotides. We have recently presented a preliminary report on the structure of the complex formed between 6-Br-9-amino-DACA and $d(CG^{5Br}UACG)_2$ (*25*), where the structure was solved by using MAD methods and synchrotron radiation. We now present a detailed analysis of the crystal structure of a complex of the parent 9-amino-DACA bound to the native hexanucleotide $d(CGTACG)_2$ that provides a molecular rationale for understanding the known structure−activity relationships for antitumor activity, that enables a mechanistic interpretation of the dependence of kinetics on ligand structure, and that suggests which determinants of the DNA−ligand complex are recognized by topoisomerase II.

EXPERIMENTAL PROCEDURES

Crystallization and Data Collection. The self-complementary deoxyribonucleotide CGTACG was synthesized on an Applied Biosystems synthesizer using phosphoramidite chemistry and the manufacturer's chemicals and protocols. It was purified using anion-exchange and reverse-phase HPLC, lyophilized as the triethylammonium salt, and dissolved in water to give a 3.3 mM stock solution which was stored frozen at 253 K. 9-Amino-DACA was synthesized as the dihydrochloride salt as previously described (*6*) and dissolved in water to give a 10 mM stock solution. Crystals were grown at 285 K by vapor diffusion in sitting drops in Cryschem 24-well crystallization plates. A 10 μL drop containing 0.5 mM DNA, 20 mM sodium cacodylate buffer, pH 6.5, 4 mM magnesium acetate, 1 mM cobalt(II) chloride, 0.33 mM spermine·4HCl, 1 mM 9-amino-DACA·2HCl, and 9% MPD was equilibrated against 1 mL of a solution of 45% MPD in water. Yellow, bullet-shaped, crystals appeared within 1 week and grew to approximately $0.3 \times 0.2 \times 0.2$ mm in 3 weeks at which time a crystal was removed from the drop, placed in Riedel de Haen perfluoropolyether RS 3000 oil, mounted in a cryoloop, and frozen at 110 K in a N_2 cryostream. Diffraction intensities were recorded on a Rigaku R-axis II image plate system mounted on a Rigaku RU-200 rotating-anode generator with focusing mirror optics (CuKα, 1.5418 Å). Data were collected in two passes at crystal-to-detector distances of 65 and 80 mm, the second being at a shorter exposure time of 5 min to allow base-pair-stacking reflections with $d \approx 3.4$ Å to be recorded accurately without overloading the image plate. The data were processed to 1.6 Å resolution with the DENZO and SCALEPACK programs (*26*) which indicated this crystal form to be in the space group $P6_4$ (or $P6_2$) with $a = 30.2$ Å and $c = 39.7$ Å (Table 1). Every 12th reflection was separated into a reference set to monitor R_{free}.

Table 1: Crystal Details, Data Collection, and Final Refinement Parameters

unit cell dimensions	$a = 30.2$ Å, $c = 39.7$ Å
space group	$P6_4$
number of observations	67055
number of unique reflections	2716
resolution range (Å)	16−1.6
R_{merge} (%)	2.9 (14.2)[a]
completeness (%)	98.4 (97.0)[a]
$I/\sigma I$	56.8 (5.0)[a]
number of atoms (non-hydrogen)	194
number of water molecules	29 (2 of which lie on the 2-fold crystallographic axis)
R_{all} (%)	19.3
R_{free} (%)	25.6
RMSD from ideal geometry of final model distances	
bonds (Å)	0.010 (0.03)[b]
angle distances (Å)	0.021 (0.05)[b]
planes (Å)	0.023 (0.10)[b]
similarity distance restraints	0.038
average B values (Å^2)	
bases	19
sugars	23
phosphates	29
intercalated 9-amino-DACA	
acridine ring	21
side chain	43
nonintercalated 9-amino-DACA	
acridine ring	17
side chain	29
water	36

[a] Values in parentheses are for last shell, 1.66−1.60 Å. [b] Target values are in parentheses.

Solution and Refinement. The hexagonal crystal form reported here is isomorphous with $R_{deriv} = 22.4\%$ to crystals of $d(CG^{5Br}UACG)_2$ complexed with the 6-bromo derivative

of 9-amino-DACA (*25*), Nucleic Acid Databank accession number DDF073. This brominated complex was refined in space group $P6_4$ (a = 30.09 Å, c = 39.32 Å) at 1.3 Å resolution with an asymmetric unit composed of a single strand of DNA, an intercalated drug molecule, and an end-stacked drug molecule. The elements of this structure chosen as a starting model for refinement were one strand of d(CGUACG)$_2$ and the chromophore of the intercalated drug molecule. The initial temperature factors were those of the brominated complex structure, and the initial R factor was 32.2% and R_{free} = 30.5% for data in the resolution shell 16−1.6 Å. An iterative refinement procedure was conducted using the program SHELXL-97 (*27*) interspersed with inspection of electron density maps and manual model rebuilding with the program O (*28*). Bond lengths and bond angles within the DNA bases were restrained to target values as specified by Taylor and Kennard (*29*). All other chemically equivalent DNA bond lengths and bond angles were restrained by similarity distance restraints but without specification of an actual target value. For 9-amino-DACA, bond lengths and bond angles were restrained to specified target values generated from an idealized structure built with INSIGHT II (*30*) and optimized with an AMBER force field using the DISCOVER program (*30*). The DNA bases, the acridine ring, and the carboxamide group of 9-amino-DACA were restrained to be planar whereas all other torsion angles remained unrestrained.

As the refinement proceeded, electron density corresponding to positions of atoms not included in the model was observed. The positions of the nonintercalated end-stacked drug and the methyl group of the thymine (uracil in initial model) could be clearly seen and were included in the model. At points where the density was unequivocal, water molecules were included, two of which were observed on the 2-fold axis. Regions of diffuse solvent were modeled using Babinet's principle as implemented in the SWAT command in SHELXL-97 (*31*). The side chains of the drugs were introduced into the refinement one at a time. For the end-stacked drug, it was clear where the side chains should be placed from both difference and the ($2F_o - F_c$) maps. For the intercalated ligand, the position of the carboxamide group and the C17 carbon atom was also clear on the difference density maps. Density for the remaining portion of the side chain was poorer, and in the ($2F_o - F_c$) maps contoured at 2.4 σ was not continuous. However, the terminal dimethylamino group could be fitted neatly into less significant density, with the refined temperature factors, which were high (mean = 52 Å), indicating some disorder. In the initial stages, tight geometrical restraints were applied to the planes (σ = 0.10 Å) of the acridine rings and the carboxamide groups of the drugs, and there was some residual difference electron density near the carboxamide group of the side chain of the intercalated ligand (*25*). Relaxing the planarity restraints on the acridine rings and carboxamide groups to a target value of σ = 0.20 Å, allowing the planes in the drug to buckle, removed all significant difference electron density. Even with the relaxed planarity restraints, the carboxamide group of the intercalated ligand remained planar (RMSD 0.004 Å). The final deviations from planarity of the intercalated acridine ring [RMSD = 0.095 Å, maximum deviation (C15) = 0.18 Å] are comparable to those observed in the crystal structure of the isolated ligand [RMSD = 0.065 Å, maximum deviation (C7) = 0.13 Å] at resolution 0.85 Å to R factor 6.2% (*22*). At the completion of refinement, the structure contains 29 water molecules with a final R factor of 19.3% and R_{free} of 25.6%. The final refinement parameters are given in Table 1. Structural parameters for the DNA were analyzed using the Curves 5.2 program (*32*).

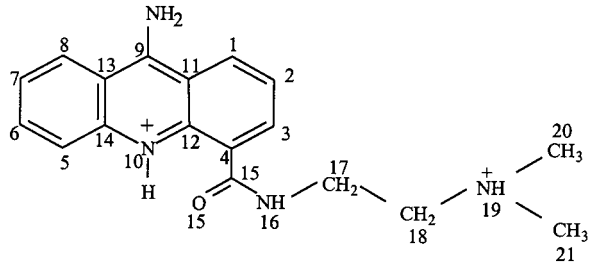

FIGURE 1: 9-Amino-DACA.

RESULTS

Global Structure and Crystal Packing. An asymmetric unit contains a single strand of DNA hexamer, 1 intercalated 9-amino-DACA molecule, 27 ordered water molecules, and an additional 9-amino-DACA and 2 water molecules located on the 2-fold axis. No metal ions or spermine are observed in the density maps. The two strands of the DNA are related by a crystallographic dyad and form a right-handed B-DNA-like duplex with Watson−Crick base pairs. The nucleotides are labeled C1 to G6 in the 5′ to 3′ direction, and the numbering scheme used for the drug is given in Figure 1. A 9-amino-DACA molecule is intercalated between each of the CpG dinucleotide base pair steps with its side chain lying in the major groove pointing toward the center of the duplex. The partially disordered protonated terminal dimethylamino group of the carboxamide side chain refines to a position within hydrogen bonding distance of the N7 and O6 atoms of guanine G2 (Figure 2 and see Figure 5). The intercalated hexanucleotide has an overall bending of 6° which shortens its end-to-end distance (23.6 Å) by 0.4% compared to its path length. The additional drug molecule on the 2-fold axis stacks on the end of each DNA helix and links it to the next duplex to form a continuous column of duplexes in the *ab* plane. The adjacent columns of duplexes are laterally well-separated by solvent, being about 12 Å apart at their edges, and thus there are no direct contacts between columns within the same plane. Since the end-stacked ligand lies on a 2-fold axis coincident with the major axis of the ligand, the polarity of the DNA backbone reverses at this point which brings the 5′ termini of adjacent helices into close juxtaposition and the cytosine C1s oppose each other across the stacked ligand (see Figure 2). As a result of this arrangement, the DNA duplexes form quasi-helical stacks with the major and minor grooves on opposite sides of the *ab* plane. The protonated *N*,*N*-dimethylamino group of the end-stacked drug makes a hydrogen bond to the N7 atom of guanine G6. The stacked columns of duplexes lie with their helical axes in planes related by a 3_1 axis parallel to *c*, the columns in neighboring planes intersecting in projection at the dyad axis. Interpenetration of helices at the dyad allows a hydrogen bond (2.9 Å) to form between neighboring columns from the 9-amino group of the intercalated drug in the minor groove to the symmetry-related phosphate group of guanine G2 (Figure 3a). There is one additional direct interstack hydrogen bond

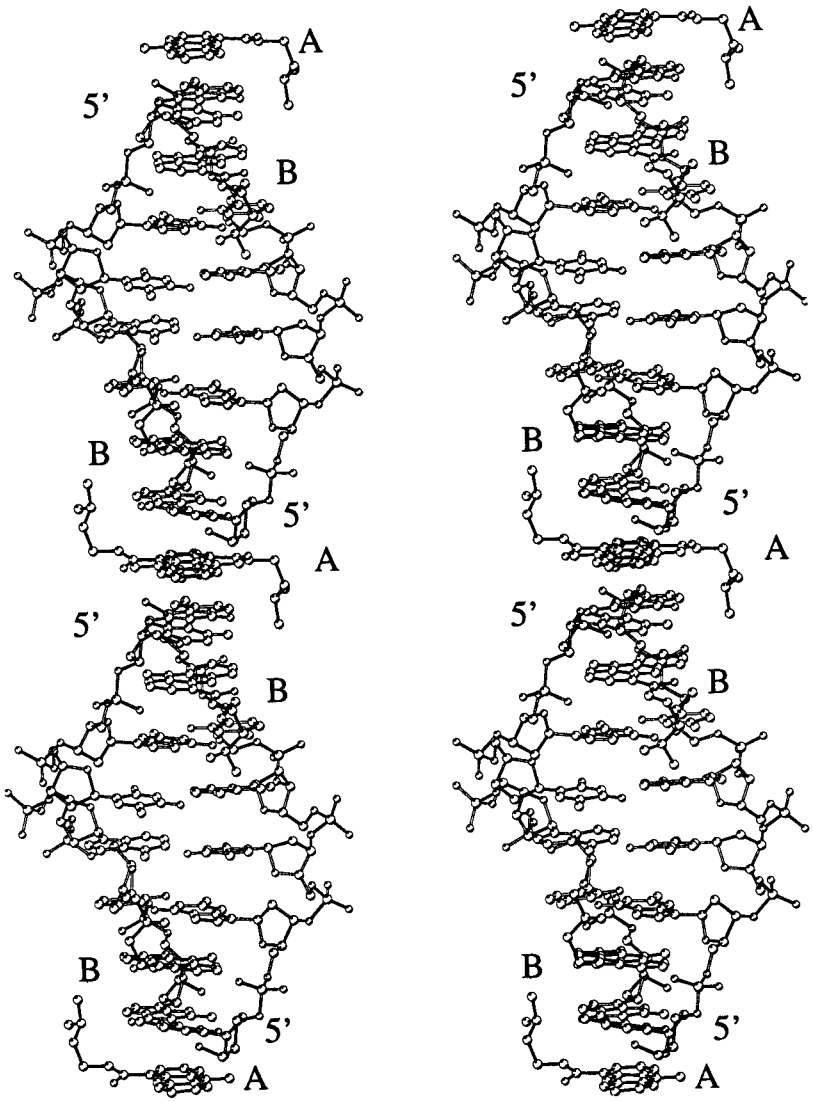

FIGURE 2: Stereoview of two bis-intercalated d(CGTACG)$_2$ hexanucleotides in the *ab* plane with the end-stacked ligand bound between them. The bonds of the ligands are drawn in black. 5′ indicates the 5′ end of each strand of the hexanucleotide. "A" indicates the positions of the end-stacked ligands and "B" the positions of the intercalated ligands.

in the structure, from the amino group of cytosine C1 in the major groove to the symmetry-related phosphate group of cytosine C5 (2.9 Å) (Figure 3b).

DNA Conformation. The DNA main chain and glycosidic torsion angles, as well as the furanose conformations, are listed in Table 2. The pseudorotation angle of cytosine C1 is 5°, indicating a C3′-*endo* sugar pucker, whereas the *P* values for all other sugar rings fall within the normal range for the C2′-*endo* pucker of 140−180°. These assignments are supported by the values of the corresponding C4′−C3′ (δ) torsion angles which are known to be correlated with sugar pucker (*33*). Thus, the sugar conformations of the nucleotides comprising the intercalation site are not all the same; that of cytosine C1 is C3′-*endo* whereas the guanines and cytosine C5 are C2′-*endo* which introduces a degree of asymmetry into the DNA backbone at the intercalation cavity. The glycosidic angles, χ, are in the *medium-anti* configuration range for C1 and G2 whereas for all other bases they are *high-anti* as is typically found in B-DNA (*33*). This further emphasizes drug-induced asymmetry at the binding site since the glycosidic angles for the bases in the 5′ strand are now different from those in the 3′ strand. With the exception of the phosphate P−O5′ and C5′−C4′ torsion angles α and γ at both guanine G2 and G6 residues, the main chain dihedral angles for all six nucleotides fall within ranges characteristic of B-DNA (*34*). At G2 and G6, the α values have rotated by 110° and 121°, respectively, compared to those of B-DNA and the γ values by 142° and 110°. These coupled α/γ rotations at the guanines are the principal modifications to the backbone torsion angles responsible for opening up the intercalation cavity. The main chain torsion angles at the GpT and ApC steps indicate each phosphate group to be in a B_I configuration, whereas the backbone dihedral angles for the TpA step are characteristic of a B_{II} phosphate conformation (*35*).

Table 3 lists the geometrical properties of the base pairs and base pair steps, and Figure 4 shows views of the three distinct base pair overlaps (step 1, C1-G2; step 2, G2-T3; and step 3, T3-A4) compared with the same projections for canonical B-DNA. For step 1, the rise of 7.0 Å is as expected for an intercalation cavity, and its twist angle shows the DNA to be unwound by 8° at the binding site. Base pair C1-G6 has a normal B-DNA propeller twist and a positive buckle of 4.0°, whereas the propeller for G2-C5 is flattened to −4°

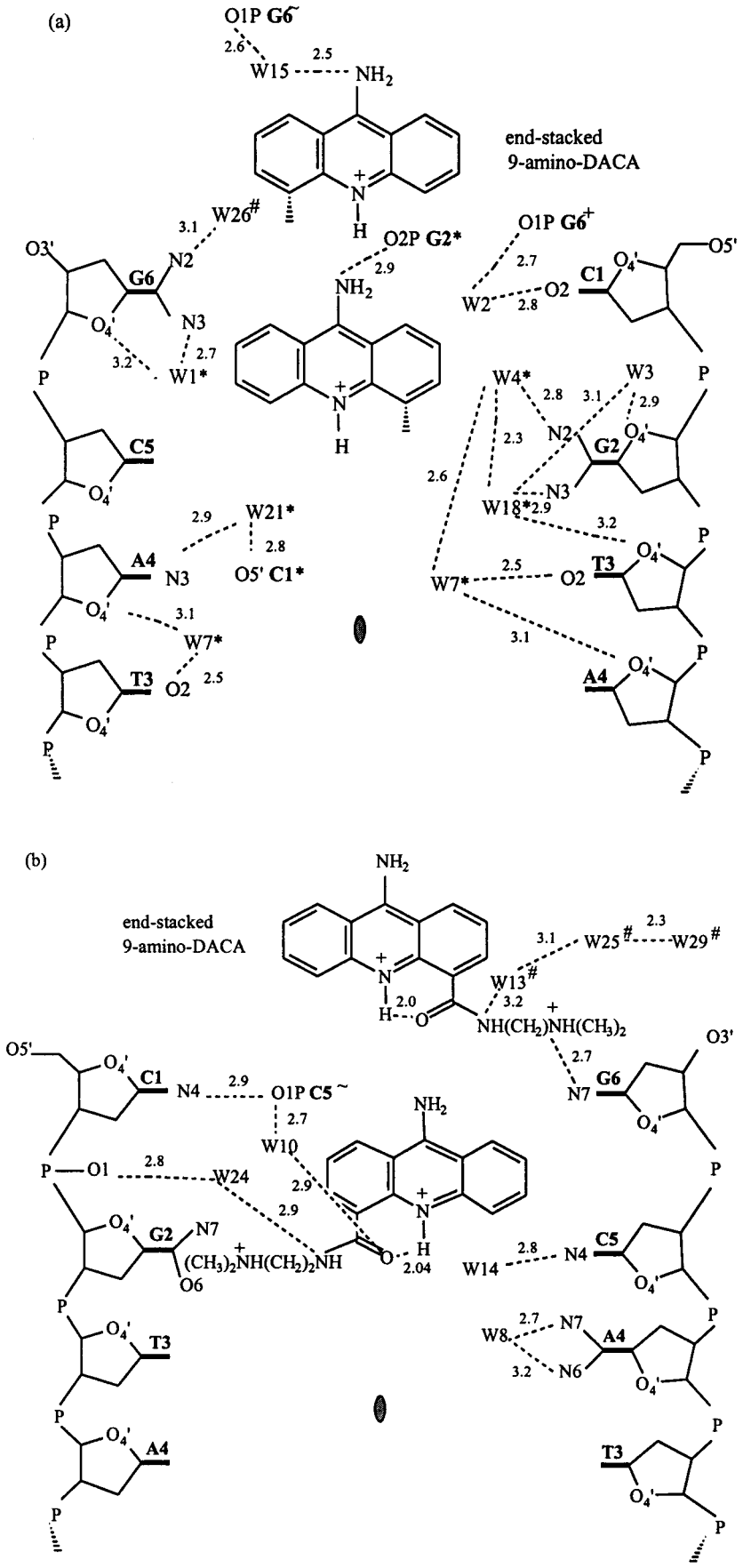

FIGURE 3: Schematic diagram showing intermolecular hydrogen bonding (dashed lines with numbers indicating distances in Å) and water structure in (a) the minor groove and (b) the major groove. Superscripted symbols denote symmetry-related molecules: (~) ($-y$, $x-y$, $z + 1/3$); (*) ($-x + y$, $-x$, $z + 2/3$); (#) ($-x$, $-y$, z); (+) (y, $-x + y$, $z + 1/3$).

Table 2: Sugar−Phosphate Torsion Angles, Glycosidic Angles (deg), and Furanose Conformations [a]

	α P−O5′	β O5′−C5′	γ C5′−C4′	δ C4′−C3′	ϵ C3′−O3′	ζ O3′−P	χ C1′−N	*P*[c]	τ_m[c]	pucker
C1			63	87	−158	−77	−136	5	40	C3′-*endo*
G2	−172	173	−170	154	−173	−100	−124	172	38	C2′-*endo*
T3	−73	−168	43	149	−126	172	−87	148	45	C2′-*endo*
A4	−63	153	50	141	175	−91	−103	158	34	C2′-*endo*
C5	−69	177	53	138	−147	−158	−90	141	39	C2′-*endo*
G6	59	164	−62	162			−75	166	41	C2′-*endo*
B DNA[b]	−62	B_I 176[c] B_{II} 146	48	B_I 128 B_{II} 144	B_I −176 B_{II} −114	B_I −95 B_{II} 174	B_IR −102 B_IY −119 B_{II} −89	160	35	C2′-*endo*

[a] All parameters were calculated using the Curves 5.2 program (*32*). [b] Average values for B-DNA taken from (*34*). [c] *P* is the pseudorotation phase angle, τ_m is the pseudorotation amplitude, and B_I and B_{II} are different phosphate conformations.

Table 3: Geometrical Properties of Base Pair Steps and Base Pairs [a]

base pair	step	shift (Å)	slide (Å)	rise (Å)	tilt (deg)	roll (deg)	twist (deg)	propeller twist (deg)	buckle (deg)
C1-G6								−12	4.0
	1	0.4	0.3	7.0	−0.6	3.8	28		
G2-C5								−4	−7.7
	2	−0.6	−0.3	3.2	0.9	1.7	24		
T3-A4								−11	2.6
	3	0.0	1.2	3.3	0.0	−1.5	53		
A4-T3								−11	−2.5
B-DNA [b]		0	0	3.4	2	1	36	−11	

[a] All parameters were calculated using the Curves 5.2 program (*32*). [b] Average values for B-DNA taken from (*33*).

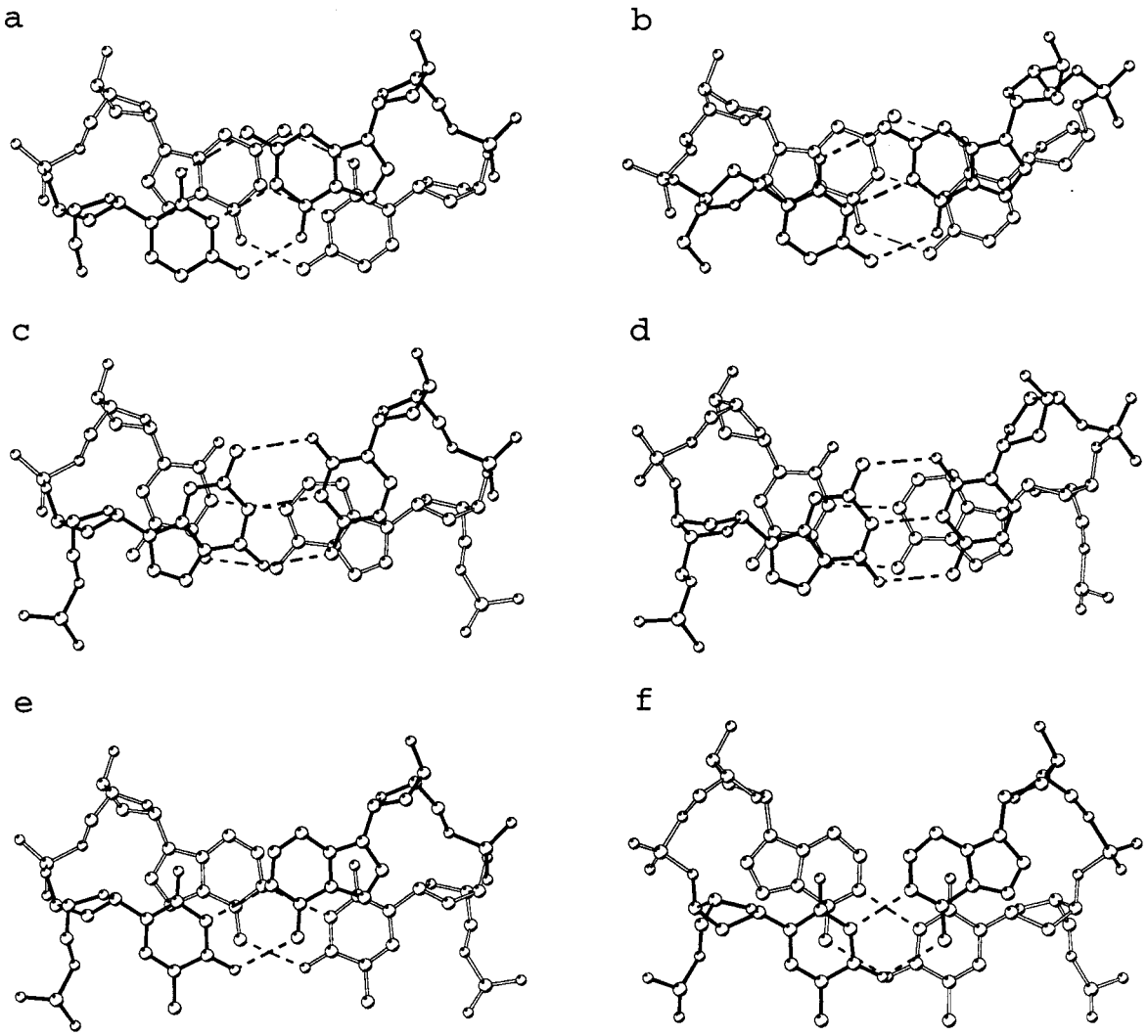

FIGURE 4: Three base pair overlaps [step 1 (b), C1-G2; step 2 (d), G2-T3; and step 3 (f), T3-A4] viewed down the helix axis compared with the same projections (a, c, and e, respectively) for canonical B-DNA.

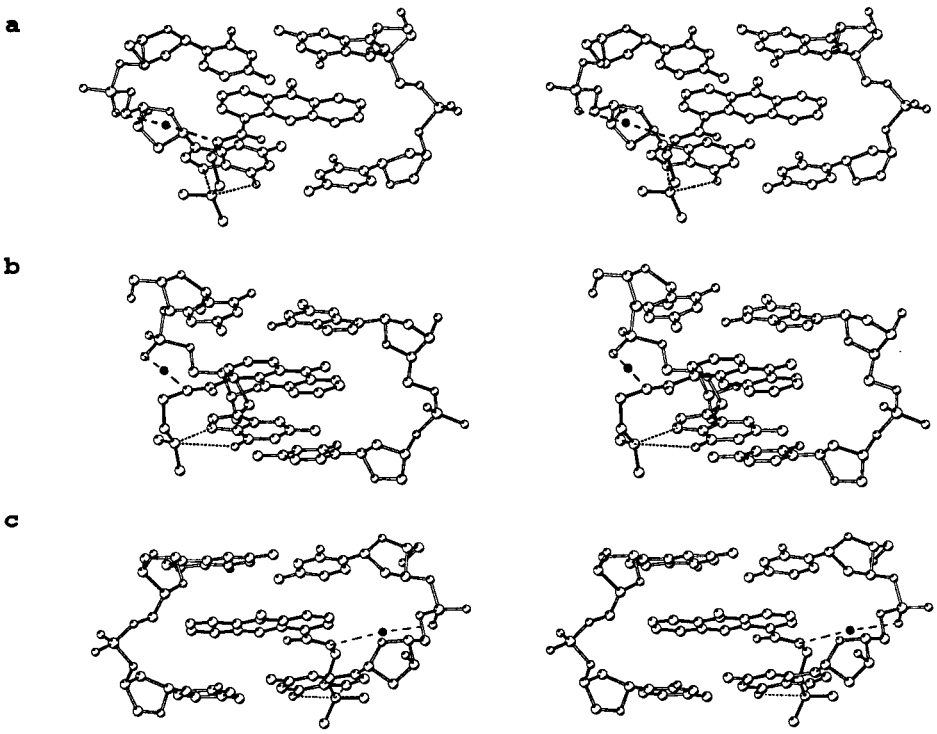

FIGURE 5: Three stereoviews of 9-amino-DACA intercalated into d(CpG)·d(GpC) and the bridging water molecule. Dashed lines indicate hydrogen bonds; dotted lines indicate distances between the O6 and N7 of guanine G2 and the refined position of the partially disordered terminal dimethylamino group. (a) Looking into the major groove; (b) 60° rotation in *y* axis from (a); (c) looking into the minor groove.

Table 4: Refined 9-Amino-DACA Side Chain Torsion Angles (deg)

	torsion angle[a]					
9-amino-DACA	1	2	3	4	5	6
intercalated[b]	9 (5)	−170 (4)	−75 (10)	−45 (10)	167 (9)	−63 (10)
end-stacked	−12 (7)	169 (7)	104 (9)	51 (9)	75 (8)	−160 (5)

[a] Torsion angle definition: 1 = C3−C4−C15−N16; 2 = C3−C4−C15−O15; 3 = C15−N16−C17−C18; 4 = N16−C17−C18−N19; 5 = C17−C18−N19−C20; 6 = C17−C18−N19−C21. [b] Torsion angles 3−6 are given for the refined position of the partially disordered terminal dimethylamino group.

and it has twice the buckle in the opposite direction. In common with base pair steps 2 and 3, step 1 has negligible tilt and a small role angle. The slide and shift parameters for step 1, which of course reflect base pair−chromophore interactions rather than base pair stacking interactions, again show the intercalation site to have elements of asymmetry as can be seen in the projections shown in Figure 4a,b. Step 2, G2-T3, has slide, shift, rise, tilt, and roll parameters typical of average B-DNA values but is unwound by 12° compared to the canonical structure. Figure 4c,d shows that G2 remains poorly stacked in the same position atop T3 as found in fiber B-DNA, whereas C5 now overlaps more of A4 so that base pair stacking is enhanced at this point in the complex. The difference from one side of the helix to the other is a result of the coupled changes in twist, shift, and slide parameters for base pairs G2-C5 and T3-A4.

In contrast to steps 1 and 2, the central T3-A4 step is overwound by 17° compared to an average B-DNA twist of 36°, and at 53° is the largest T−A twist observed in any B-DNA crystal analysis to date (*36*). Although the propeller and buckle angles are typical of B-DNA at this step, the overwinding forces the base pairs to slide out of the helical stack in order to prevent a steric clash between the edges of the two adenine bases across the helix. As can be seen in Figure 4e,f, these two maneuvers bring the O4 oxygens (2.9 Å) and C5 methyl groups (5.7 Å) of the two thymines close together in the major groove, and leave the base pairs with minimal overlap of their aromatic rings. However, favorable base pair interactions are still facilitated, since now the thymine O2 oxygens lie over the six-membered ring of the adenines and the 6 amino groups of the adenines lie over the center of the thymine rings in what is quite a symmetrical arrangement (Figure 4f).

Intercalated 9-Amino-DACA Conformation and DNA Interactions. Figure 5 shows stereoviews of 9-amino-DACA intercalated via the major groove of the d(CpG)·d(GpC) binding site which illustrate a number of important features of the complex. The 4-carboxamide group is planar, with the carbonyl oxygen forming an internal hydrogen bond to the protonated acridine ring nitrogen (see Table 4 for side chain dihedral angles). This interaction, coupled with a drive to maximize resonance stabilization energy between the carboxamide and the acridine chromophore, allows the carboxamide group to lie within 9° of the acridine plane (cf. *22*). In this configuration, the carboxamide NH group points toward the sugar−phosphate backbone where it hydrogen bonds (2.9 Å) to a water molecule which in turn hydrogen bonds (2.8 Å) to the phosphate group of guanine G2 (Figure 5). A $[2F_o - F_c]$ electron density map defining the water-bridged hydrogen bonding interactions is shown in Figure

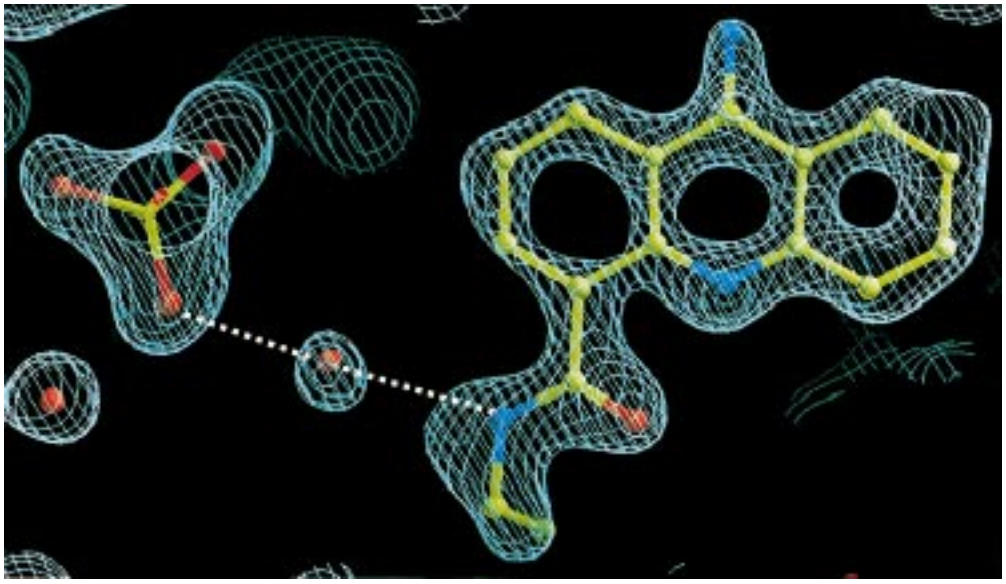

FIGURE 6: Electron density ($2F_o - F_c$) map in the area of the intercalated ligand with the positions of the hydrogen bonds from water molecule 24 to N16 of the ligand and to a phosphate oxygen of G2 indicated by dashed white lines.

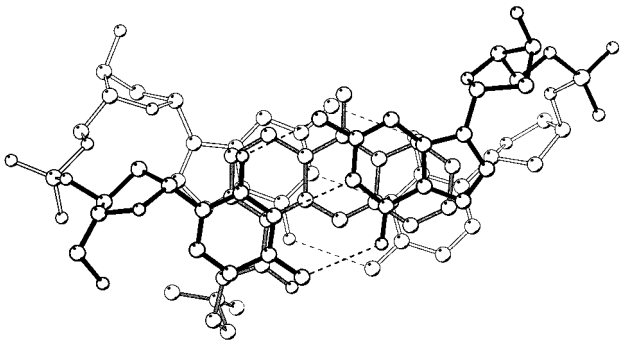

FIGURE 7: Projection down the helix axis of a d(CpG)·d(GpC) dinucleotide with sandwiched intercalated ligand. The GC base pair C1-G6 (on top) is drawn with dark bonds. The ligand has gray bonds.

6. In the refined conformation of the partially disordered portion of the side chain, the protonated *N*,*N*-dimethylaminoethyl moiety projects at right angles to the plane of the acridine ring, placing the ammonium group within hydrogen bonding distance of the N7 nitrogen (3.1 Å) and the O6 oxygen (3.1 Å) of guanine G2 (see Table 4 and Figures 3b and 5). The 9-amino group of the intercalated drug, which lies in the minor groove, forms no interactions with the DNA at the intercalation site, although, as mentioned above, it hydrogen bonds with a symmetry-related duplex (see Figure 3a).

The stacking interactions between intercalated ligand and the DNA bases are shown in projection in Figure 7, where it can be seen that the acridine is aligned with its major axis bisecting the angle between the hydrogen bonds of the sandwiching base pairs. The helix axis passes through the middle of the central acridine ring. The acridine chromophore is practically enveloped by the two base pairs, and the three atoms of the 4-carboxamide group are neatly stacked on the C4, O4, and C5 atoms of cytosine C1. In this way, the chromophore comes to be positioned as close as possible to the helix axis and is deeply buried in the helical stack. The acridine C5 and C6 positions, which are important sites for substitution from a biological and kinetic perspective (*7, 8, 20*), are stacked on cytosine C5.

End-Stacked 9-Amino-DACA Conformation and DNA Interactions. Figure 8a shows a stereoview of an end-stacked 9-amino-DACA molecule sandwiched between the C1-G6 base pairs of two symmetry-related hexanucleotides in the quasi-continuous stack. A second, symmetry-related, ligand molecule is superimposed on the first, but flipped over along its major axis. As with the intercalated ligand, the 4-carboxamide group is planar, and the carbonyl oxygen forms an internal hydrogen bond to the protonated acridine ring nitrogen (see Table 4). The carboxamide group lies within 12° of the acridine plane, and the side chain projects at right angles to the plane of the chromophore in an extended conformation (Table 4). However, compared to the intercalated ligand, the side chain C17−C18 bond is rotated by about 90° in the direction that swings the dimethylamino group toward the DNA backbone, and the C18−N19 bond is rotated about 90° in the opposite direction so as to facilitate a strong hydrogen bond (2.7 Å) between the protonated amine and the N7 atom of guanine G6. The 4-carboxamide NH group is hydrogen bonded to water W13# which is in turn H-bonded to W29# via W25# (see Figure 3b). Water W15 forms a hydrogen-bonded bridge between the ligand 9-amino group and the phosphate group of guanine G6 in a symmetry-related duplex (see Figure 3a). In projection down the helix axis (Figure 8b), the stacking pattern shows a high degree of symmetry with the base pairs forming an arrangement reminiscent of an arrowhead, pointing to the left of the figure. The acridine rings overlap the cytosine bases and the six-membered rings of the guanines and are well-enveloped by the base pairs.

Water Structure Not Involving Ligand Molecules. Very little ordered water is found associated with the base pairs in the DNA major groove. Water W8 forms bridging hydrogen bonds to the N7 nitrogen and the 6-amino group of adenine A4, and the amino group of cytosine C5 hydrogen bonds to water W14 (Figure 3b). In contrast, there are more substantial DNA−water networks in the minor groove (Figure 3a). Five waters interconnect the pyrimidine O2 oxygens, the purine N3 nitrogens, the guanine 2-amino group, and the furanose O4′ oxygens from cytosine C1 through

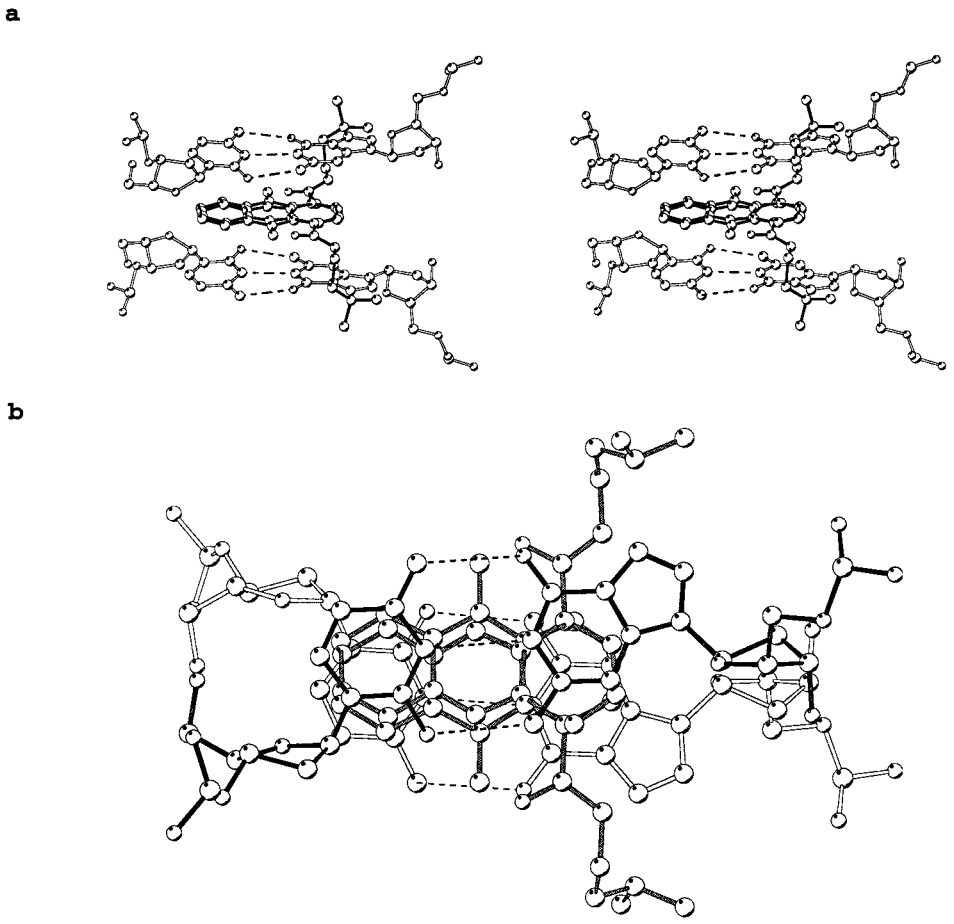

FIGURE 8: End-stacked ligand bound between contiguous C1-G6 base pairs: (a) stereoview, the ligand is drawn with dark bonds; (b) in projection down the helix axis, the top C1-G6 base pair has dark bonds, the ligand gray bonds.

adenine A4. The water molecules at the ends of this ribbon form bridges to the phosphate group of guanine G6 and the terminal O5′ hydroxyl of cytosine C1 on symmetry-related duplexes, respectively. Cytosine C5 has no discernible attached waters. Two water molecules bind to the 2-amino group, the N3 and the O4′ atoms of guanine G6. No waters are found located around the phosphate groups, presumably because they are disordered.

DISCUSSION

Carboxamide Side Chain−DNA Interactions in the Intercalated Complex. The work reported here provides the first direct experimental evidence for the binding orientation of 9-amino-DACA and unequivocally demonstrates that the 4-carboxamide side chain lodges in the major groove at CpG sequences. From a drug development perspective, our most significant findings relate to the conformation adopted by the 4-carboxamide group, to the involvement of a bridging water molecule between the carboxamide NH and the phosphate at the intercalation site, and to the putative hydrogen-bonding interactions of the protonated dimethylammonium group with the O6 and N7 atoms of guanine. The key element controlling side chain−DNA interactions is the formation of the internal hydrogen bond between the carboxamide carbonyl group and the protonated N10 nitrogen of the acridine ring which, coupled with resonance stabilization effects, holds the carboxamide in the plane of the intercalated chromophore. The possibility of this interaction was first noted by Hudson et al. (*22*) although it failed to be a feature in their molecular model of the 9-amino-DACA/d(CpG)$_2$ complex. With the carboxamide constrained to the intercalation plane, and confined to its orientation by the internal hydrogen bond and the phosphate-bridging water molecule, the *N*,*N*-dimethylaminoethyl moiety lies toward the edge of the major groove close to the O6 and N7 atoms of guanine. Of the molecular modeling studies, that by Rehn and Pindur (*23*) best resembles the crystal structure, with its prediction of the three-centered hydrogen bond between the alkylammonium group and the guanine O6/N7 atoms. It would appear that the high molecular electrostatic potential in the vicinity of the guanine O6 and N7 atoms (*37*, *38*) and the strong nucleophilicity of the latter (*37*) are important determinants in defining both binding groove orientation and sequence selectivity for 9-amino-DACA. Its strong preference for binding to GC-rich sequences in DNA restriction fragments is consistent with the proposed hydrogen bonding scheme (*18*). The nature of the observed disorder in the position of the *N*,*N*-dimethylaminoethyl portion of the side chain in the crystal structure indicates that the ammonium head is in dynamic equilibrium with the protonated N−H oscillating between interaction with the guanine O6 and N7 atoms.

DNA Conformation in the Intercalated Complex. In accommodating an intercalated 9-amino-DACA, the DNA assumes conformational parameters significantly different from average B-DNA values. At the intercalation site, the sugars of cytosine C1 and guanine G2 adopt the conformation C3′-*endo*, C2′-*endo*, a configuration frequently found in

intercalator/dinucleotide monophosphate complexes (*39*), and the glycosidic angles are *medium-anti*, whereas on the complementary strand both sugars remain C2′-*endo* with *high-anti* χ values, as do all the other sugars in the hexanucleotide. Thus, at the intercalation site, the structure is heteronomous, a maneuver which permits the C2 and C3 edges of the acridine ring closer approach to the DNA backbone and facilitates the side chain−guanine interaction. The 7 Å intercalation cavity has largely been created by coupled "crank-shaft" rotations of the α/γ main chain torsion angles at guanines G2 and G6 which additionally result in the unusual situation where both phosphate O3′ and O5′ oxygen atoms point toward the minor groove. The helix unwinding angle of 17° measured with covalently closed circular DNA in solution (*16*) is seen to be spread over several base pair steps in the crystal structure. Compared to the canonical value of 36°, the intercalation site itself is unwound by 8° and the GpT step by 12°, and, in contrary fashion, the TpA step is *overwound* by 17°, giving a net unwinding angle per bound ligand molecule in the crystal of 12°. Extrapolating to an isolated ligand bound in polymeric DNA of sequence ...TACGTA... would predict an unwinding angle of 15° (+8.5° −12° −8° −12° +8.5°) if the overwinding at the TpA step in the crystal structure is apportioned equally between bound ligands. The transmission of helical distortions beyond the intercalation site is especially emphasized at the TpA step where the overwinding is accompanied by changes in the phosphate geometry from the normal B_I to the B_{II} conformation which rotates the O3′ oxygen inward toward the helix axis. In addition, to avoid cross-strand collisions between adenines due to the overwinding, the AT base pairs slide out of the helical stack, and their aromatic rings are virtually unstacked from each other. The minor groove width at the TpA step is 6.5 Å, which is the normal value for B-DNA, and suggests that this type of conformational change may lie at the heart of the enhanced cleavage by DNase I seen at AT-rich sequences between 9-amino-DACA-binding sites in footprinting measurements (*18*).

DNA−Ligand Stacking Interactions and Water Structure in the Intercalated Complex. The positively charged acridine has penetrated deeply into the helical stack so as to form strong hydrophobic interactions with the base pairs and to locate its center of mass as close to the helix axis as possible where the negative molecular electrostatic potential of the DNA is greatest (*38*, *40*). In this way, the chromophore comes to lie in a position where both its hydrophobic and its electrostatic interactions with the DNA are maximized. Of course, the equilibrium position of the acridine ring ultimately represents a balance between these forces and the geometrical requirements to form the intermolecular interactions involving the 4-carboxamide side chain. The intercalated complex is also stabilized indirectly by the chain of ordered water molecules that extends from the O2 oxygen of cytosine C1 down the minor groove to the N3 atom of adenine A4. The general characteristic of these water molecules is that they form bridging hydrogen bonds between hydrogen bonding atoms on the bases and the furanose O4′ oxygen of the next nucleotide 3′ along the sequence. Thus, they form a network connecting a base to the next sugar in the sequence, the hydrogen bonding energy of which presumably contributes to stabilizing the particular DNA conformations that we observe. The contribution of water W7 may be particularly important in this regard since it is strongly bound between the O2 oxygen of thymine T3 and the furanose O4′ of adenine A4, and most likely helps stabilize the overwinding at the TpA step.

Carboxamide Side Chain Interactions of the End-Stacked Ligand. The side chain−DNA interactions of the end-stacked 9-amino-DACA molecule are subtly different from those of the intercalated ligand. For the end-stacked ligand, although the carboxamide group retains the internal hydrogen bond to the protonated acridine N10 atom and lies essentially in the plane of the chromophore, the torsion angles around the ethyl portion of the side chain direct the protonated terminal N−H group to hydrogen bond selectively and strongly to the guanine N7 atom. It is not clear whether this difference in behavior of the two ligands is related to the greater degree of freedom of the chromophore in the end-stacked situation or to the presence of the phosphate-bridging water molecule for the intercalated ligand, or whether it is a consequence of the fact that the end-stacked ligand binds 3′ to the guanine whereas the intercalated one stacks on the 5′ side of the guanine to which it is hydrogen bonded. Interestingly, in the related crystal structure of the 6-Br-9-amino-DACA/d($CG^{5Br}UACG$)$_2$ complex (*25*), the end-stacked ligand is unprotonated, despite the fact that the acridine pK_a of the brominated free ligand is 6.8 and the pH of crystallization is 6.5. In this case, the N−H group of the carboxamide now makes a hydrogen bond to the N10 nitrogen of the acridine, thus rotating the carboxamide group by 180° compared to that found here. This transformation draws the *N*,*N*-dimethylaminoethyl portion of the side chain closer to the helix axis; nevertheless, the dimethylammonium cation succeeds in making a strong hydrogen bond (2.8 Å) to the terminal guanine (*25*).

Comparison with Crystal Structures of Other DNA−Ligand Complexes. In comparing the structure of the intercalated complex presented here with that of 6-Br-9-amino-DACA/d($CG^{5Br}UACG$)$_2$ (*25*), it appears that the bromine atoms in the DNA and ligand have little effect on the conformation of the DNA, with the main chain torsion angles, sugar puckers, and winding angles being very similar. However, the conformation of the side chain differs somewhat in the two structures, with the carbon atom of the carboxamide group in the brominated ligand taking on elements of tetrahedral geometry, although the carboxamide group still hydrogen bonds to the acridine N10−H and the phosphate-bridging water molecule (*25*). It is not clear why the two complexes should differ in this way. The difference may be related to the electronic and steric effects of the bromine atom in position 5, or possibly it is a consequence of the different resolution of the two structures (1.3 Å for the bromo derivative compared to 1.6 Å for the native structure). An additional, and possibly important, difference, however, is the finding that the protonated dimethylammonium group of the brominated ligand does not form a multicentered interaction with the O6 and N7 atoms of guanine G2 but is hydrogen bonded solely to the guanine N7 atom.

The work presented here and that of Todd et al. (*25*) are the first reported crystal structures of an acridine bound to a nucleic acid substrate larger than a dinucleotide. Sakore et al. (*41*) found that 9-aminoacridine intercalates into iodoCpG

with maximum chromophore−base pair overlap and its 9-amino group located in the minor groove of the incipient mini RNA helix. In contrast to the paucity of crystal structures of acridine−DNA complexes, there are more than 40 structures of DNA complexes of the anthracycline topoisomerase poisons in the Nucleic Acid Data Base (*42*). All are complexes with hexanucleotides in which a drug molecule intercalates at each terminal pyrimidine-3′,5′-purine site, the long axis of its chromophore lying perpendicular to the major axis of the base pairs and its sugar positioned in the minor groove. The helical unwinding in DNA−anthracycline complexes is confined to the intercalation step, and the overwinding that we observe for the central TpA step in the 9-amino-DACA complex is not seen. Similarly, the geometry of the intercalation cavity differs for the two ligand classes with the anthracyclines generally causing a base pair separation of 5−6 Å at the binding site compared to a rise of 7 Å in the 9-aminoacridine−4-carboxamide complexes. Moreover, since the anthracyclines "spear" the DNA duplex, leaving a gap on either side of their chromophores within the intercalation cavity, the bases lining the cavity buckle to fill the empty space (*43*−*47*), a phenomenon not observed in our structure since the major axis of the 9-aminoacridine chromophore aligns itself parallel to the major axes of the base pairs so as to maximally occupy the intercalation site. Opening the intercalation cavity to its maximal separation of 7 Å to facilitate base pair−chromophore stacking interactions in this way has necessitated major changes to the sugar−phosphate backbone in the 9-amino-DACA complex, namely, the coupled α/γ rotations, which are absent in the anthracycline complexes whose sugar−phosphate backbone geometry is similar to that of B-DNA (*43*−*47*).

Rationalization of Structure−Activity Relationships for Antitumor Activity and DNA-Binding Kinetics. This work provides the first opportunity for interpreting the structure−activity relationships for biological activity among 9-aminoacridine-4-carboxamides in terms of a defined molecular structure for the DNA complex of the parent ligand. Previous studies with analogues of 9-amino-DACA revealed the importance of both the position and nature of the carboxamide side chain for cytotoxicity, antitumor activity, and the kinetic stability of the DNA complex formed (*6*−*8*, *20*). Only compounds bearing a 4-CONH$(CH_2)_2$NRR side chain show significant cytotoxicity and antitumor activity: moving the side chain to the 2- or 3-position gives inactive analogues. These findings are consistent with the crystal structure since, substituted in positions 2 and 3, the acridine ring cannot intercalate fully so as to maximize its stacking interactions with the base pairs and, at the same time, present the side chain in the correct position for interacting with the O6/N7 atoms of guanine. Methylating the carboxamide unit to give a −CON(Me)− moiety, or replacing it with a sulfonamide, $-SO_2NH-$, or extending the methylene chain to $-(CH_2)_3-$ or longer lead to much lower cytotoxicity and abrogates antitumor activity. These effects can now be seen to be related to the fact that, by steric interaction with the hydrogen in position 3, the *N*-methyl group prevents the carboxamide from being coplanar with the acridine ring and displaces binding of the bridging water molecule to the phosphate at the intercalation cavity, that the sulfonamide geometry is inappropriate for maintaining both the internal hydrogen bond and the bridging water molecule in the correct positions, and that by extending the methylene chain the dimethylammonium group is less well-positioned for interacting with the O6 and N7 atoms of guanine.

In distinction to these very tight structure−activity relationships, a wider range of modifications can be tolerated in the nature of the terminal amine substituents. That the methyl groups can be replaced by ethyl or hydroxyethyl groups with moderate effects on biological activity can now be understood, since there is room in the major groove of the DNA complex to accommodate these larger alkyl groups without disturbing the side chain−guanine interactions. However, there are limits to the acceptable size of the ammonium substituents since the morpholino derivative, despite being able to fit in the DNA groove and participate in the putative hydrogen bonding interaction (see below), is biologically inactive. These latter findings hint at the importance of additional intermolecular interactions of the *N*,*N*-dimethylammonium group with the topoisomerase. Substituting the acridine ring with chlorine, methyl, and methoxy groups reveals a structure−activity pattern where substituents are tolerated in the 1-, 2-, 5-, and 6-positions (*7*). The crystal structure shows that substituents in the 1- and 2-positions lie in the minor groove without obstructing the DNA backbone and that the 5 and 6 substituents are positioned in the major groove, again without unfavorable steric interactions. In contrast, substituents in the 3-, 7-, and 8-positions are sharply deleterious to biological activity, and in the case of the 7 and 8 substituents this is clearly due to steric collision with the sugar−phosphate backbone. Substituents in position 3 have many ways of antagonizing formation of the active DNA complex: they sterically prevent the carboxamide group from lying in the plane of the chromophore, they displace the phosphate-bridging water molecule, and they may also collide directly with the sugar−phosphate backbone.

In their studies of the relationships between DNA-binding kinetics and biological activity for the 9-aminoacridine-4-carboxamides, Wakelin and colleagues (*20*) found that 9-amino-DACA dissociates from calf thymus DNA with a complex kinetic profile comprising four exponential components. The structural modifications described above, with the exception of the morpholino substitution, that lead to loss of cytotoxic potency and antitumor activity also lead to loss of the fourth, and slowest, kinetic transient (*20*). Wakelin et al. (*20*) speculated that the slowest transient is associated with a specific interaction of the 4-carboxamide side chain with the DNA bases that is characteristic of the biologically active form of the bound drug. The kinetic results were interpreted at the time in terms of a proposed binding model in which the side chain lay in the minor groove, with the carboxamide NH and the protonated dimethylammonium groups both making hydrogen bonds to the O2 oxygen of a cytosine at the CpG-binding site (*20*). However, in light of the crystal structure, the correlations between ligand structure and kinetic profile suggest that the fourth transient is actually related to interactions between the ammonium group and guanine O6/N7 atoms in the major groove.

The structure−activity relationships, the crystal structure, and the kinetic findings taken together focus attention on the interaction between the dimethylammonium group and the O6/N7 atoms of guanine as the critical determinant that leads to poisoning of topoisomerase II. Clearly, this is an

important interaction that presumably prevents the enzyme from making essential hydrogen bonds to guanine. However, the evidence suggests that the 4-carboxamide side chain does more than simply prevent access to guanine O6/N7 atoms since the nature of the terminal ammonium group does modulate biological activity. Since this can be accomplished without disruption of the interaction between the ammonium group and guanine, a conclusion emphasized by the morpholino derivative which maintains the kinetic profile of 9-amino-DACA yet is devoid of antitumor activity (*20*), this implies that the *N*,*N*-dimethyl groups play a part in binding to the protein in the ternary complex. That substituents in the acridine 5-position markedly enhance biological activity suggests that such potential intermolecular interactions might also extend to the acridine ring itself (*7*, *8*). Thus, it seems likely that topoisomerase poisoning results from the combined loss of access to the O6/N7 atoms of guanine and formation of a ternary complex involving intermolecular interactions that encompass the full face of the drug in the major groove of the intercalated complex.

Relevance of the Structure of the 9-Amino-DACA/d(CGTACG)$_2$ Complex to the Binding Modes of DACA and Amsacrine-4-carboxamide. Making the 9-amino-DACA chromophore neutral by removing the 9-amino group, or substituting further to give phenazine, promotes activity against solid tumors (*14*, *48*). Kinetic studies show that the DNA complexes of both DACA and the phenazine-4-carboxamide exhibit dissociation profiles similar to those of 9-amino-DACA, each having transients comprising four components, the slowest one of which is lost on extending the length of the alkyl side chain (Wakelin and Denny, unpublished observations). Thus, it appears that the dimethylammonium group in these ligands is also capable of hydrogen bonding to the DNA bases. In the crystal structure of the free base of 9-amino-DACA, the NH group of the carboxamide makes an internal hydrogen bond to the acridine N10 atom (*22*), a configuration also found in the "end-stacked" form of 6-Br-9-amino-DACA bound to d(CG^{5Br}UACG)$_2$ (*25*) where the dimethylammonium group hydrogen bonds to the N7 of guanine at the ends of the duplex. Thus, with the evidence at hand, it seems probable that DACA and the phenazine-4-carboxamide bind to DNA in an analogous way to 9-amino-DACA by intercalating from the major groove with their carboxamide groups in the plane of the chromophore and their dimethylammonium groups interacting with the O6/N7 atoms of guanine. The amsacrine-4-carboxamides are a class of DNA threading agent derived from 9-anilinoacridine that possesses similar biological properties to amsacrine and 9-amino-DACA (*49*). The parent compound bears an *N*,*N*-dimethylaminoethyl-4-carboxamide side chain and is potently cytotoxic, has experimental antitumor activity, poisons topoisomerases I and II, intercalates into DNA, positioning the anilino group in one groove and the 4-carboxamide side chain in the other, and binds selectively to GC-rich DNA sequences (9, *18*, *49*−*53*). Kinetic measurements indicate that its 4-carboxamide side chain−DNA interactions are of the same type as those found for 9-amino-DACA which lead the authors to suggest that the two compounds bind with the same orientation (*50*, *51*). Thus, the current work suggests that the carboxamide side chain of amsacrine-4-carboxamide lies in the major groove, making hydrogen bonding interactions with the O6/N7 atoms of guanine, and that its 9-anilino group lies in the minor groove.

ACKNOWLEDGMENT

We thank Madeleine H. Moore and Charles S. Bond for helpful discussions and are grateful to Christine J. Cardin and Alan K. Todd, who made available the coordinates of the structure of 6-bromo-9-amino-DACA complexed with d(CG^{5Br}UACG)$_2$ prior to their release by the Nucleic Acid Database (*25*).

REFERENCES

1. Malonne, H., and Atassi G. (1997) *Anti-Cancer Drugs 8*, 811−822.
2. Denny, W. A. (1997) *Exp. Opin. Invest. Drugs 6*, 1845−1851.
3. Baguley, B. C., Denny, W. A., Atwell, G. J., Finlay, G. J., Rewcastle, G. W., Twigden, S. J., and Wilson, W. R. (1984) *Cancer Res. 44*, 3245−3252.
4. Harvey, V. J., Hardy, J. R., Smith, S., Grove, W., and Baguley, B. C. (1991) *Eur. J. Cancer 27*, 1617−1620.
5. Sklarin, N. T., Wiernik, P. H., Grove, W. R., Benson, L., Mittelman, A., Maroun, J. A., Stewart, J. A., Robert, F., Doroshow, J. H., and Rosen, P. J. (1992) *Invest. New Drugs 10*, 309−312.
6. Atwell, G. J., Cain, B. F., Baguley, B. C., Finlay, G. J., and Denny, W. A. (1984) *J. Med. Chem. 27*, 1481−1485.
7. Rewcastle, G. W., Atwell, G. J., Chambers, D., Baguley, B. C., and Denny, W. A. (1986) *J. Med. Chem. 29*, 472−477.
8. Denny, W. A., Atwell, G. J., Rewcastle, G. W., and Baguley, B. C. (1987) *J. Med. Chem. 30*, 658−663.
9. Finlay, G. J., Riou, J.-F., and Baguley, B. C. (1996) *Eur. J. Cancer 32A*, 708−714.
10. Schneider, E., Darkin, S. A., Lawson, P. A., Ching, L.-M., Ralph, R. K., and Baguley, B. C. (1988) *Eur. J. Cancer Clin. Oncol. 24*, 1783−1790.
11. Baguley, B. C., Zhuang, L., and Marshall, E. M (1995) *Cancer Chemother. Pharmacol. 36*, 244−248.
12. Kestell, P., Dunlop, I., McCrystal, M. R., Evans, B. D., Paxton, J. W., Gamage, R. S. K. A., and Baguley, B. C. (1999) *Cancer Chemother. Pharmacol. 44*, 45−50.
13. McCrystal, M. R., Evans, B. D., Harvey, V. J., Thompson, P. I., Porter, D. J., and Baguley, B. C. (1999) *Cancer Chemother. Pharmacol. 44*, 39−44.
14. Atwell, G. J., Rewcastle, G. W., Baguley, B. C., and Denny, W. A. (1987) *J. Med. Chem. 30*, 664−669.
15. Finlay, G. J., Marshall, E. S., Matthews, J. H. L., Paull, K. D., and Baguley, B. C. (1993) *Cancer Chemother. Pharmacol. 31*, 401−406.
16. Palmer, B. D., Rewcastle, G. W., Baguley, B. C., and Denny, W. A. (1988) *J. Med. Chem. 31*, 707−712.
17. Crenshaw, J. M., Graves, D. E., and Denny, W. A. (1995) *Biochemistry 34*, 13682−13687.
18. Bailly, C., Denny, W. A., Mellor, L. E., Wakelin, L. P. G., and Waring, M. J. (1992) *Biochemistry 31*, 3514−3524.
19. Denny, W. A., Roos, I. A. G., and Wakelin, L. P. G. (1986) *Anti-Cancer Drug Des. 1*, 141−147.
20. Wakelin, L. P. G., Atwell, G. J., Rewcastle, G. W., and Denny, W. A (1987) *J. Med. Chem. 30*, 855−862.
21. Chen, K.-X., Gresh, N., and Pullman, B. (1987) *FEBS Lett. 224*, 361−364.
22. Hudson, B. D., Kuroda, R., Denny, W. A., and Neidle, S. (1987) *J. Biomol. Struct. Dyn. 5*, 145−158.
23. Rehn, C., and Pindur, U. (1996) *Monatsh. Chem. 127*, 645−658.
24. Woodson, S. A., and Crothers, D. M. (1988) *Biochemistry 27*, 8904−8914.
25. Todd, A. K., Adams, A., Thorpe, J. H., Denny, W. A., Wakelin, L. P. G., and Cardin, C. J. (1999) *J. Med. Chem. 42*, 536−540.
26. Otwinowski, Z. (1993) Oscillation data reduction program. in *Proceedings of the CCP4 Study Weekend: Data Collection*

and Processing (Sawyer, L., Isaacs, N., and Bailey, S. S., Eds.) pp 56−62, SERC, Daresbury Laboratory, Warrington, U.,K.
27. Sheldrick, G. M. (1997) *The SHELX-97 Manual*, University of Göttingen.
28. Jones, T. A., Zou, J. Y., Cowan, S. W., and Kjeldgaard, M. (1991) *Acta Crystallogr. A47*, 110−119.
29. Taylor, R., and Kennard, O. (1982) *J. Am. Chem. Soc. 104*, 3206−3212.
30. *Insight II User Guide* (1995) Biosym/MSI, San Diego.
31. Moews, P. C., and Kretsinger, R. H. (1975) *J. Mol. Biol. 91*, 201−225.
32. Lavery, R., and Sklenar, H. (1989) *J. Biomol. Struct. Dyn. 6*, 655−667.
33. Neidle, S. (1994) *DNA Structure and Recognition* (Rickwood, D., Ed.) IRL Press at Oxford University Press, Oxford, U.K.
34. Schneider, B., Neidle, S., and Berman, H. M. (1997) *Biopolymers 42*, 13−124.
35. Fratini, A. V., Kopka, M. L., Drew, H. R., and Dickerson, R. E. (1983) *J. Biol. Chem. 257*, 14686−14707.
36. Goodsell, D. S., Kaczor-Grzeskowiak, M., and Dickerson, R. E. (1994) *J. Mol. Biol. 239*, 79−96.
37. Pullman, A., and Pullman, B. (1981) *Q. Rev. Biophys. 14*, 289−380.
38. Dean, P. M., and Wakelin, L. P. G. (1980) *Proc. R. Soc. London, Ser. B 209*, 453−471.
39. Neidle, S., and Abraham, Z. (1984) *CRC Crit. Rev. Biochem. 17*, 73−121.
40. Nuss, M. E., and Kollman, P. A. (1979) *J. Med. Chem. 22*, 1517−1524.
41. Sakore, T. D., Reddy, B. S., and Sobell, H. M. (1979) *J. Mol. Biol. 135*, 763−785.
42. Berman, H. M., Olson, W. K., Beveridge, D. L., Westbrook, J., Gelbin, A., Demeny, T., Hsieh, S.-H., Srinivasan, A. R., and Schneider, B. (1992) *Biophys. J. 63*, 751−759.
43. Gao, Y.-G., and Wang, H.-J. (1995) *J. Biomol. Struct. Dyn. 13*, 103−117.
44. Frederick, C. A., Williams, L. D., Ughetto, G., van der Marel, G. A., van Boom, J. H., Rich, A., and Wang, A. H.-J. (1990) *Biochemistry 29*, 2538−2549.
45. Wang, A. H.-J., Ughetto, G., Quigley, G. J., and Rich, A. (1987) *Biochemistry 26*, 1152−1163.
46. Smith, C. K., Davies, G. J., Dodson, E. J., and Moore, M. H. (1995) *Biochemistry 34*, 415−425.
47. Dautant, A., Langlois d'Estaintot, B., Gallois, B., Brown, T., and Hunter, W. N. (1995) *Nucleic Acids Res. 23*, 1710−1716.
48. Rewcastle, G. W., Denny, W. A., and Baguley, B. C. (1987) *J. Med. Chem. 30*, 843−851.
49. Denny, W. A., Atwell, G. J., and Baguley, B. C. (1984) *J. Med. Chem. 27*, 363−366.
50. Wakelin, L. P. G., Chetcuti, P., and Denny, W. A. (1990) *J. Med. Chem. 33*, 2039−2044.
51. Wakelin, L. P. G., and Denny, W. A. (1990) in *Molecular Basis of Specificity in Nucleic Acid−Drug Interactions* (Pullman, B., and Jortner, J., Eds.) pp 191−206, Kluwer Academic Publishers, Dordrecht.
52. Bailly, C., Denny, W. A., and Waring, M. J. (1996) *Anti-Cancer Drug Des. 11*, 611−624.
53. Searcey, M., McClean, S., Madden, B., McGown, A. T., and Wakelin, L. P. G. (1998) *Anti-Cancer Drug Des. 13*, 837−855.

BI990352M